Optical properties of CrO_2, MoO_2, and WO_2 in the range 0.2–6 eV

M. A. K. L. Dissanayake* and L. L. Chase
Department of Physics, Indiana University, Bloomington, Indiana 47401
(Received 19 May 1978)

The dielectric functions and optical conductivities of CrO_2, MoO_2, and WO_2 have been obtained from reflectivity measurements, and the results are interpreted on the basis of qualitative models proposed for the band structures of the transition-metal dioxide series. CrO_2 has been studied as a function of temperature above and below its ferromagnetic transition at $T_c = 392$°K. Three conductivity peaks are observed to shift substantially near T_c, and a band near 0.8 eV in the ferromagnetic phase is assigned to transitions between exchange-split Cr d bands. An increase in $3d$ bandwidth and $2p$-$3d$ separation is observed in the sequence CrO_2, VO_2, MoO_2, and WO_2, and these effects are correlated with an increasing cation radius. No evidence is found for greatly differing bandwidths for $3d$ orbitals of different symmetries, as has been proposed on empirical grounds.

I. INTRODUCTION

There has been a great deal of experimental and theoretical activity aimed at understanding the electronic structure of transition-metal dioxides, particularly the structure of the cationic d bands. The dioxides of V, Cr. Mo, and W are some of the most suitable oxides for a systematic investigation of the d-band structure, because of the similarity in their crystal structure and the diversity in electrical and magnetic properties. VO_2 has been subjected to extensive investigations in recent years because of the semiconductor-metal phase transition observed at 340°K. However, the detailed structure of the $3d$ bands and the role played by electron correlations and electron-phonon interactions on the phase transition of this material is still not well established. With a $3d^2$ outer-electron configuration, CrO_2 is an interesting material because of its metallic behavior and the ferromagnetic-paramagnetic phase transition observed at 392 °K, although it does not show large changes in its transport properties at the phase transition.[1] MoO_2 and WO_2 have $4d^2$ and $5d^2$ outer-electron configurations and are metallic and weakly paramagnetic at all temperatures.[2,3] CrO_2 has the tetragonal (rutile) structure of metallic VO_2 whereas MoO_2 and WO_2 have monoclinic structure similar to semiconducting VO_2. Therefore, it should be interesting to study the optical properties of these materials in order to understand the nature of the cationic d bands which appears to be primarily responsible for the diverse nature of the observed physical properties.

The room-temperature optical properties of CrO_2 and MoO_2 have been previously investigated.[4] It was suggested that the similar conductivity peaks observed at 0.8 eV in both materials could result from quasiparticle absorption due to the correlation-induced Hubbard splitting of the cationic d bands. The absorption peak observed at 1 eV in VO_2 has been subjected to a similar interpretation.[5] There remains, however, the possibility of normal interband transitions within the cationic d bands which could account for the appearance of the conductivity peaks around 1 eV in these materials.

In this paper we report the temperature dependence of the optical properties of CrO_2 from 77 °K up to 450 °K and compare the room-temperature optical properties of MoO_2 and WO_2 in the energy range of 0.2–6.0 eV. In the absence of detailed energy-band calculations for CrO_2, MoO_2, and WO_2, we shall refer to Goodenough's qualitative energy-band schemes[6] for the interpretation of our optical data. We find in the present investigation that the ordinary interband transitions within the cationic d bands alone could account for the nature of the low-energy conductivity peak in these oxides.

II. EXPERIMENTAL PROCEDURE

The preparation of CrO_2 films and MoO_2 single crystals used in the reflectivity measurements has been described previously.[4] Single crystals of WO_2 were grown using a vapor transport technique similar to that used for growing MoO_2 crystals.[7] A ratio-recording, double-beam reflectometer, consisting of a Spex model 1500 spectrometer, deuterium, tungsten, and globar sources, and phototube and thermopile detectors was used to measure the near-normal incidence reflectivity spectra of the samples from 2000 Å up to 7 μm. Separate chopping frequencies were used for signal and reference arms of the spectrometer. Further details of the optical and electronic arrangements are given in Ref. 8. The data were collected

on a point by point basis using the continuous scanning mode of the spectrometer and automatic triggering of the recording electronics at switch-selected wavelength intervals. In the visible and uv regions an electronic feedback arrangement was used to control the high voltage applied to the phototube so that the output of the reference-channel lock-in amplifier remains constant. The ratio of the intensitites in the sample and reference channels was recorded by a teletype and processed with the calibration data to obtain the complete reflectivity spectra. In the case of CrO_2 our attempts to collect data above 450 °K were not successful because of the tendency of the CrO_2 samples to dissociate into Cr_2O_3 at these temperatures. In collecting the low-temperature data the sample was sealed in helium gas inside a specially designed sample holder which was attached to the cold finger of the cryotip of an optical Dewar. Calcium fluoride windows were used both in the sample holder and in the optical Dewar to allow for the passage of light. In spite of many precautions, we observe a slight drop in the relative magnitude of the reflectivity at low temperature in the uv region. Most probably this is due to a contamination of the CaF_2 window used in the sample holder. The regions of the spectrum which are most likely to be affected by such contamination are indicated by dashed lines in the figures. The data on CrO_2 were taken with incident light parallel and perpendicular to the rutile c axis. However, due to the smaller size of the samples, the measurements on MoO_2 and WO_2 were taken with unpolarized light and were limited to room temperature only. The angular dependence of the reflectivity of all three materials was measured using helium-neon and argon-ion lasers and the reflectivity data were Kramers-Krönig analyzed to obtain the dielectric functions and the optical conductivities following the procedure described previously.[4]

III. EXPERIMENTAL RESULTS

The optical conductivities of CrO_2 shown in Fig. 1 are obtained from a Kramers-Krönig analysis of the reflectivity data with an extrapolating parameter $p = 2.00$ in the extrapolation function

$$R(E) = R(E_{\max})(E_{\max}/E)^p \quad \text{for } E > E_{\max}, \tag{1}$$

where $E_{\max} = 6.0$ eV is the upper cut off energy. The structures observed in the room-temperature spectra are consistent with the data reported earlier.[4] There is a well-defined low-energy conductivity peak at $E_1 \simeq 0.8$ eV which can be associated with the reflectivity shoulder around 1 eV. Other conductivity peaks in the room-temperature

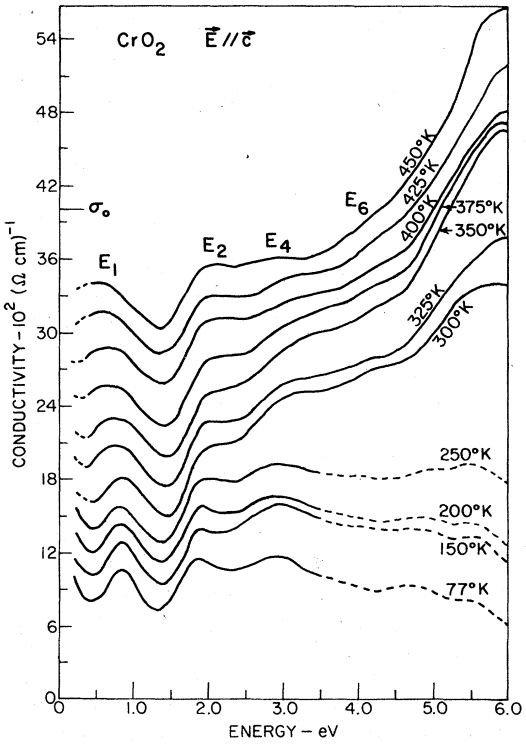

FIG. 1. Temperature dependence of the $\vec{E} \| \vec{c}$ optical conductivity of CrO_2 obtained from the Kramers-Krönig analysis of reflectivity data.

spectrum appear at $E_2 \simeq 2$ eV, $E_4 \simeq 3.1$ eV, and $E_6 \simeq 4.2$ eV. The conductivity at the E_1 peak is about 1.2×10^3 $(\Omega\text{cm})^{-1}$ which is much smaller than the reported dc conductivity of $\sigma_0 \simeq 4 \times 10^4$ $(\Omega\text{cm})^{-1}$.

The low-energy conductivity peak E_1 exhibits a red shift with increasing temperature from about 0.85 eV at 77 °K to about 0.5 eV at 450 °K and a particularly noticeable change occurs in the vicinity of the Curie point. This red shift is accompanied by a gradual broadening of the peak. However, the intensity of this peak does not show a significant change with temperature. The conductivity peak E_2 around 2 eV shifts from about 1.85 eV at 77 °K to about 2.10 eV at 450 °K with increasing temperature. The peak E_4 around 3 eV shifts to lower energies by about 0.2 eV as the temperature is increased from 77 °K up to 450 °K. We have observed corresponding changes in the $\vec{E} \perp \vec{c}$ conductivity spectrum.[8]

The unpolarized, room-temperature reflectivity spectra of MoO_2 and WO_2 single crystals are shown in Fig. 2. In the reflectivity spectrum of MoO_2 there is a marked, low-energy peak around 0.8 eV. The data reported earlier shows a broad shoulder at this energy. This difference may be due to different orientations of the crystal in the two

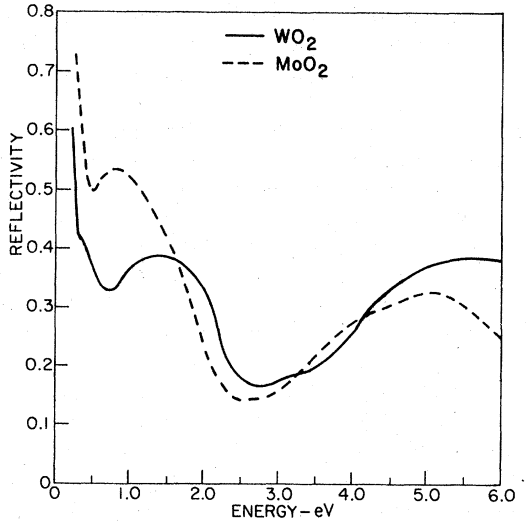

FIG. 2. Unpolarized reflectivity spectra of MoO_2 and WO_2 at 300 °K.

measurements. The optical conductivity, obtained by a Kramers-Krönig analysis of the reflectivity data with an extrapolating parameter $p = 2.7$ in Eq. (1), is shown in Fig. 4. The intense conductivity peak A at 0.8 eV is associated with the low-energy reflectivity peak around the same energy. The conductivity at this peak is about 2.1×10^3 $(\Omega\text{cm})^{-1}$ which is much smaller than the reported dc conductivity of $\sigma_0 \simeq 10^4$ $(\Omega\text{cm})^{-1}$. A weak structure A_2 at 2.6 eV is apparent in the conductivity spectrum. The most intense, broader peak at higher energy appears to exhibit a double-peak character with A_3 at 4.0 eV and A_4 at 4.5 eV. The energies of these structures are found to be consistent with the data reported earlier.[4]

The reflectivity spectrum of WO_2, shown in Fig. 2, looks quite similar to that of MoO_2 in its general characteristics. The low-energy peak observed at about 1.5 eV is broader than the corresponding peak in the reflectivity spectrum of MoO_2. There is also a broad maximum around 5 eV which appears to exhibit a double-peak character. The dielectric functions shown in Fig. 3 and the optical conductivity shown in Fig. 4 are obtained by a Kramers-Krönig transformation of the reflectivity spectrum with an extrapolating parameter $p = 1.3$ in Eq. (1). Two intense conductivity peaks appear at $E_2 = 1.75$ eV and $E_5 \simeq 5.5$ eV. There are also three faint structures at $E_1 = 0.5$ eV, $E_3 = 3.25$ eV, and $E_4 = 4.3$ eV. It is interesting to note that the conductivity at the peak E_1 and E_2 are both greater than the reported dc conductivity of $\sigma_0 \simeq 500$ $(\Omega\text{cm})^{-1}$ for this material, a feature which distinguishes WO_2 from CrO_2, metallic VO_2 and isoelectronic MoO_2.

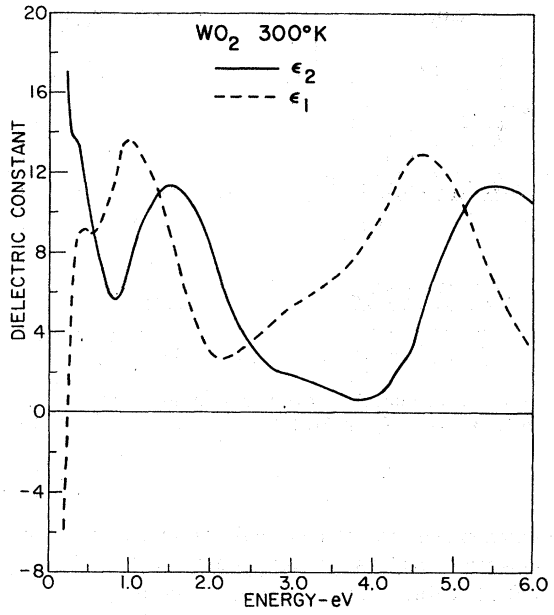

FIG. 3. Real and imaginary parts of the dielectric constant of WO_2.

IV. DISCUSSION

A detailed analysis of the optical results on CrO_2, MoO_2, and WO_2 is not possible at present because there are no band-structure calculations available for these materials. However, it is possible to interpret much of the observed data by comparing it with corresponding optical data on VO_2 and with the phenomenological models proposed by Goodenough.[6]

On the basis of the symmetry arguments and

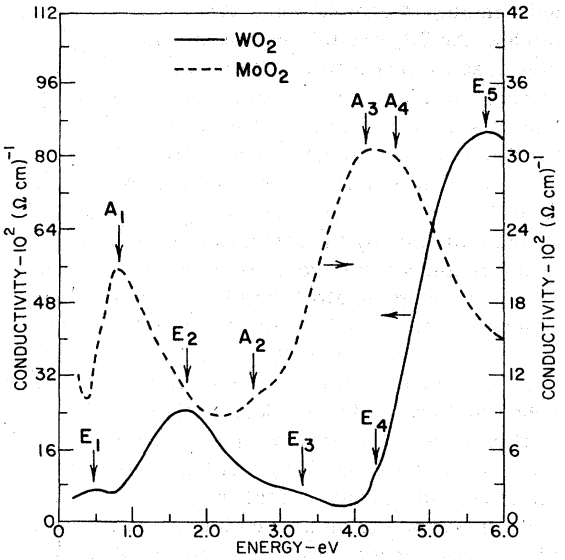

FIG. 4. Optical conductivity spectra of MoO_2 and WO_2.

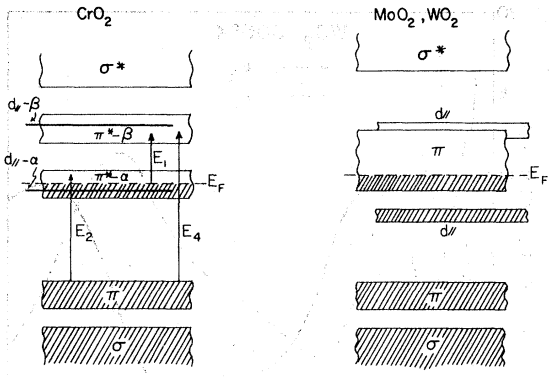

FIG. 5. Schematic energy band diagrams of CrO_2, MoO_2, and WO_2 from Ref. 6.

known trends in the physical properties of transition-metal oxides Goodenough has outlined the essential features of the energy-band diagrams of the rutile structure family of transition-metal dioxides.[6] In CrO_2 the fivefold degenerate d levels of the Cr^{4+} ion are split by the crystal field. The octahedral field of the six near-neighbor oxygens splits the d levels into a low-lying triply degenerate state of t_{2g} symmetry and a higher-lying, doubly degenerate state of e_g symmetry. The degeneracies of these states are further removed by the orthorhombic component of the crystalline field giving rise to two $3d_\sigma$ orbitals, two $3d_\pi$ orbitals, and a $3d_\parallel$ orbital as shown in Fig. 5. Covalent mixing between the oxygen $2p_\pi$ and chromium $3d_\pi$ orbitals oriented perpendicular to the rutile c axis is presumed to give rise to bonding π and antibonding π^* bands, while the two $3d_\sigma$ orbitals form antibonding σ^* bands. According to Goodenough's model, the $3d_\parallel$ orbitals oriented along the c axis give rise to localized $d_\parallel$ states in CrO_2, and the intra-atomic exchange interaction splits the $d_\parallel$ and π^* states into states of different spin. A similar model can explain the simultaneous occurence of metal-metal doublets and metallic conductivity in MoO_2 and WO_2.[6] According to this model, the $d_\parallel$ band is split by the formation of metal-metal doublets along the c axis, as in semiconducting VO_2. However, in MoO_2 and WO_2, one d electron is used for the metal-metal σ bonding and the other d electron is used to partially fill the metal-oxygen π^* band. This gives rise to the metallic behavior in these two oxides. Although this general picture of the energy bands is based on qualitative considerations, it provides a basis for an interpretation of our optical data.

The presence of an absorption edge around 1.5 eV in CrO_2 suggests that this energy separates the Fermi level in the d bands from the top of the primarily anionic valence band. The absorption peaks at higher energies are generally attributed to transitions from the valence band to the cationic d bands. Structures below 1.5 eV are most likely associated with free-carrier absorption and electronic transitions between cationic d bands. The appearance of similar conductivity peaks around 1 eV in VO_2, V_2O_3, CrO_2, and MoO_2 has been a subject of speculation in the last few years.[4,5,9] These conductivity peaks are associated with the low-energy reflectivity shoulders or peaks around 1 eV and are possibly the results of electronic transitions between the cationic d bands.

There are several possible mechanisms that might account for the presence of a conductivity peak at 1 eV in these transition-metal oxides. Some of the mechanisms have already been discussed earlier.[4] The observed changes of the energy position of the E_1 conductivity peak in CrO_2 with increasing temperature, particularly in the vicinity of the Curie point, suggests that the ferromagnetic interactions play an important role in that material. The red shift of the E_1 conductivity peak and the accompanying changes exhibited by the higher-energy conductivity peaks as the temperature is increased near and above T_C can be adequately explained on the basis of Goodenough's energy-band scheme shown in Fig. 5. According to this scheme, the intra-atomic exchange splitting of the partially filled π^* and $d_\parallel$ bands into α (spin-up) and β(spin-down) bands, leaves the π^*-α band half filled and the $d_\parallel$-α band completely filled. Therefore, interband transitions between the up-spin and down-spin π^* bands could give rise to the low-energy conductivity peak E_1 observed in this material. The change in the band gap between the up-spin and down-spin subbands split by the ferromagnetic exchange interaction would be proportional to the molecular field $J\langle S_z\rangle$ where J is the exchange interaction and $\langle S_z\rangle$ is the average of the localized spin components. The study of the magnetic properties of CrO_2 has shown that the magnetization follows the Brillouin function[12] with change in temperature, although local ordering may lead to a different dependence for $\langle S_z\rangle$ in a particular cell. As the temperature is increased toward T_C, the increasing spin disorder is expected to lead to a narrowing of the exhange-split band gap between the up-spin and down-spin subbands. Therefore, the red shift exhibited by the E_1 conductivity peak is consistent with the assignment of this peak to interband transitions between the up-spin and the down-spin cationic subbands, as illustrated in Fig. 5.

A thermomagnetic curve of CrO_2 taken from the work of Siratori and Iida[12] is reproduced in Fig. 6 for the purpose of comparison with the observed

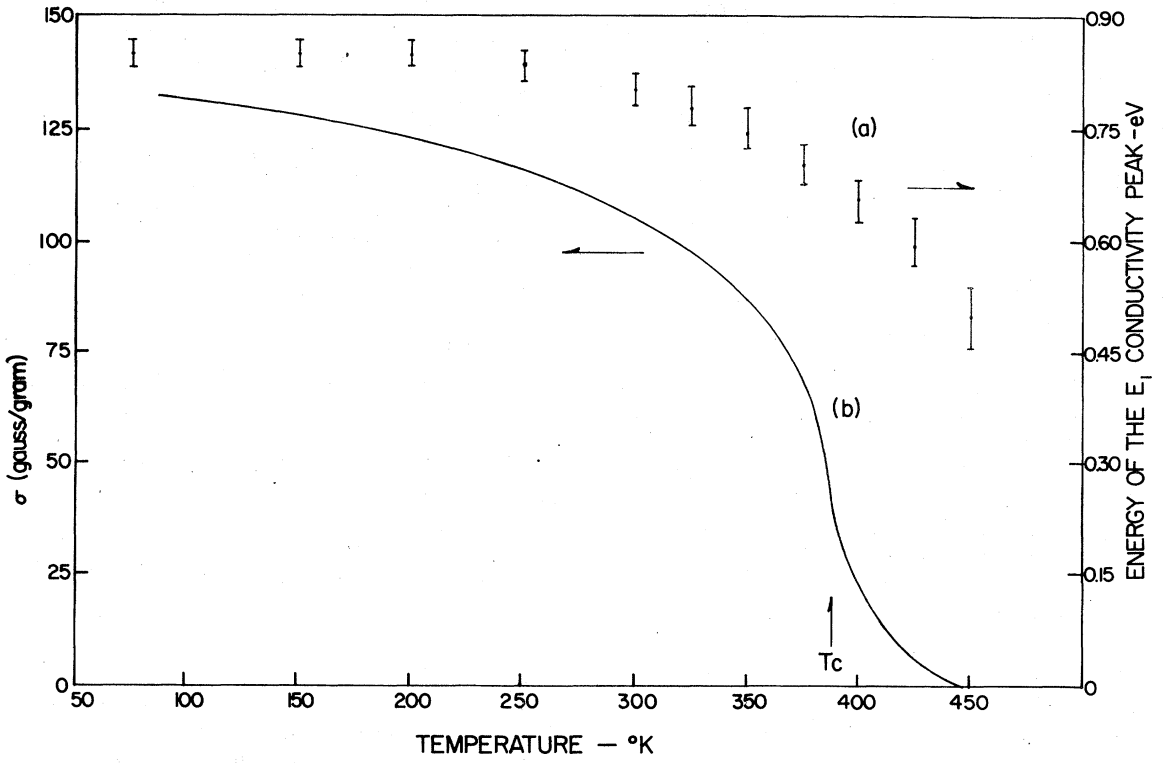

FIG. 6. (a) Variation of the energy of the E_1 conductivity peak in CrO_2 with temperature (experimental points). (b) Temperature dependence of magnetization of ferromagnetic CrO_2 taken from the work of Siratori and Iida (Ref. 12) (solid curve).

temperature dependence of the energy position of the E_1 conductivity peak. The rapid decrease in the energy of the E_1 peak near and above T_C observed in our optical data appears to be consistent with the disappearance of the magnetization in that temperature region. However, according to our observations, the E_1 peak does not go to zero energy at T_C as does the magnetization. This may be due to short-range spin correlations which can persist well above T_C, but it might also be possible that completely overlapping up-spin and down-spin π^* bands at higher temperatures could give rise to a nonzero energy for the E_1 conductivity peak. The optical data on CrO_2, therefore, appears to be consistent with the assignment of the E_1 conductivity peak to ordinary interband transitions between the up-spin and down-spin cationic subbands split by the ferromagnetic exchange interaction. This appears to be the most likely interpretation of the observed data because it has the virtue of explaining the rapid change in the energy of the E_1 peak near the Curie point.

It is important to point out one basic feature of Goodenough's proposed cationic d-band structure of CrO_2 which is not revealed in our observations. The $d_{\|}$ states proposed in the model are presumed to be localized because the length of the c_r axis is larger than the empirically derived critical separation needed for the conduction in the $d_{\|}$ bands. These localized $d_{\|}$ states are also expected to be split by the ferromagnetic exchange interaction similar to the collective electron π^* bands. In Fig. 5 the localized $d_{\|}$-α and $d_{\|}$-β levels are shown superposed on the π^*-α and π^*-β bands. Therefore, one should expect the optical reflectivity spectrum of CrO_2 to show a sharp structure around 1 eV, superposed on the low-energy reflectivity shoulder, due to the optical transitions between the exchange split $d_{\|}$ levels. Our observations, however, do not reveal the presence of such a structure, even in the thermomodulated spectra.[8] Therefore, it can be concluded that there is no substantial difference in the widths of the $d_{\|}$ and π^* bands in CrO_2.

Although ordinary interband transitions are capable of explaining the nature of the E_1 conductivity peak in CrO_2, there exist two alternative mechanisms which could give rise to a low-energy conductivity peak around 1 eV. One is an interband absorption between two quasiparticle subbands split by the electronic correlation effect. This possibility is more likely in narrow-band

materials such as many transition-metal oxides. However, the observed temperature dependence of the energy of the E_1 peak makes it difficult to interpret the data on the basis of electron correlation effects.

The second alternative mechanism that might account for the presence of a conductivity peak around 1 eV in CrO_2 would be the absorption of light by small radius polarons.[4,10] In fact, the absorption peak at 0.8 eV observed in semiconducting rutile (TiO_2) has been interpreted as due to light absorption by small polarons.[11] Our observations show, however, that the temperature dependence of the width of the E_1 conductivity peak in CrO_2 does not follow the same type of variation as expected for polaron absorption.[8] Also, the observed value of the conductivity at the E_1 peak, 1.2×10^3 $(\Omega\,\mathrm{cm})^{-1}$, is much smaller than the reported dc conductivity of this material in contrast with the polaron absorption. The shift to lower energy of the E_1 peak with increasing temperature is further evidence against the possibility of polaron absorption.

The conductivity peaks in CrO_2 above the absorption edge of 1.5 eV should be due to interband transitions between the $2p_\pi$ valence band of oxygen and the $3d$ conduction band of chromium. In Goodenough's model the terminal states are the anionic π band and the up-spin and down-spin bands originating from the chromium $3d$ bands. The presence of an absorption edge at 1.5 eV suggests that the Fermi level in the up-spin conduction band is above the top of the π valence band by this energy. The E_2 conductivity peak shifts from ~1.85 to ~2.10 eV as the temperature is raised from 77 to 450 °K. The relative variation follows a pattern similar to that observed in the low energy conductivity peak, E_1. Assignment of the E_2 peak to optical transitions from the π band to the α-spin band is therefore consistent with the narrowing of the exchange-split d band gap with increasing temperature. Such a narrowing with increasing spin disorder causes the α-spin band to be raised relative to the π-valence band, thereby accounting for the observed blue shift of the E_2 conductivity peak. The $\vec{E} \parallel \vec{c}$ conductivity peak at ~3 eV can similarly be assigned to optical transitions between the π-valence band and the β-spin band. The observed red shift of the ~0.2 eV of this peak would then be consistent with the lowering of the β-spin band relative to the valence band, as the temperature is increased through and above T_C. Thus the combined behavior of the conductivity peaks E_1, E_2, and E_4 with increasing temperature is consistent with a narrowing of the d-band gap in CrO_2 caused by the disappearance of the long-range magnetic order.

The optical results of MoO_2 and WO_2 reported here are intended mainly for comparison with the optical data of CrO_2 and VO_2.[9,13] It is again useful to rely upon a phenomenological energy-band scheme, such as that proposed by Goodenough[6] and illustrated in Fig. 5, in order to analyze the experimental data. According to this scheme, the collective-electron $d_\parallel$ state is assumed to be split by the formation of cation-cation homopolar bonding along the c axis, as in semiconducting VO_2. This leaves one electron per MoO_2 molecule in the bonding $d_\parallel$ state and the other electron per MoO_2 molecule in the π^* band.

The conductivity spectrum of MoO_2 shows a rise in the optical absorption above ~2.5 eV suggesting that this energy separates the highest oxygen p band from the Fermi level in the $4d$ bands. The optical properties of MoO_2 at energies up to 2 eV are dominated by the conduction-electron response and a single absorption band. This absorption band presumably leads to the lowest-energy reflectivity peak around 0.8 eV and the well defined, intense conductivity peak at 0.8 eV. Although it is difficult to assign this conductivity peak to possible interband transitions within the molybdenum $4d$ bands without knowing the detailed structure of the d bands, it may be attributed to one or more of the following transitions. These are filled $d_\parallel \rightarrow$ empty $d_\parallel$, filled $d_\parallel \rightarrow$ half filled π^*, and half filled $\pi^* \rightarrow$ empty $d_\parallel$ transitions. Comparison with the assignment of low-energy conductivity peaks in semiconducting VO_2 (Refs. 9 and 14) suggests that the filled $d_\parallel$ bands are involved in the transitions. From the observed width of the 0.8-eV conductivity peak in MoO_2 it is clear that the d bands involved in the transitions are not very narrow. This is supported by the optical effective mass of $m^* \simeq 5m_e$ estimated by Chase[4] assuming one carrier per cation.

The general characteristics of the optical properties of WO_2 are quite similar to those of MoO_2. The absorption edge around 4 eV and the peak at 5.5 eV can be associated with p to d transitions with the Fermi level lying above the top of the highest oxygen p bands by about 4 eV. The broad, intense conductivity peak at $E_2 \simeq 1.75$ eV is most likely to be associated with a d to d transition within the tungsten $5d$ bands. The conductivity peak is broader and more intense compared to the corresponding 0.8 eV peak in MoO_2, suggesting that the d bands involved in the transition are also broader in WO_2 than in MoO_2.

It is interesting to compare the major features of the optical spectra of the three oxides in order to gain a better understanding of any systematic correlations that might exist in their electronic structures. The low-energy reflectivity shoulder

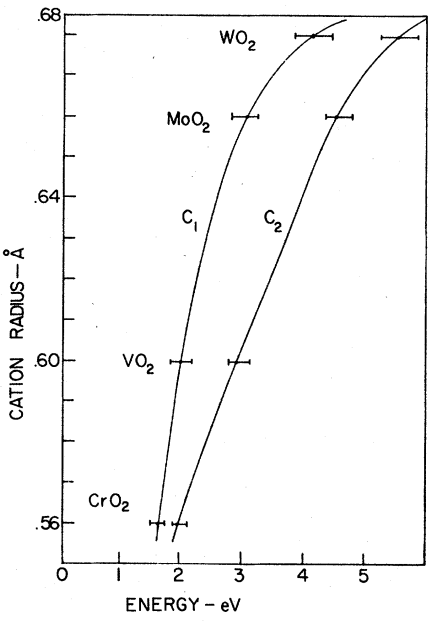

FIG. 7. Variation of the p-d charge-transfer absorption edge (curve C_1) and the p-d charge-transfer absorption peak (curve C_2) with the cation radius.

or peak becomes broader and more pronounced and the corresponding conductivity peak becomes broader and more intense in the sequence $CrO_2 \rightarrow MoO_2 \rightarrow WO_2$. The energy of this conductivity peak seems to follow a similar sequence. The p-d charge-transfer absorption peak and the absorption edge, which is a measure of the p-d band separation, appears to exhibit a definite trend towards an increase of the p-d separation with increasing cationic radius. Also the width and the intensity of the p-d absorption peak increase in the same sequence. These trends are illustrated in Fig. 7, where the positions of the p-d absorption edge and the peak of the absorption band are plotted as a function of cation radius. The c/a ratio also decreases monotonically from 0.66 for CrO_2 to 0.566 for WO_2 in this same sequence. These variations appear to be consistent with the trend indicated by Wilson[15] on the basis of qualitative considerations. The 4d and 5d electrons, being less tightly bound energetically and spatially than 3d electrons, are more directly exposed to ligands. Therefore, they are expected to show greater d-p mixing giving rise to an enlarged d-band width. The observed broadening of the low-energy (~1 eV) conductivity peak with increasing cationic radius seems to be consistent with such a trend. The broadening of the higher-energy p-d absorption peak in the same sequence may also reflect the overall broadening of the cationic d bands with increasing cationic radius. For the purpose of this comparison, plots of the p-d band gap energy and the p-d absorption edge, as obtained from our optical data, are shown in Fig. 7 as a function of the cationic radius.

V. CONCLUSIONS

From the study of the optical reflectivity spectrum and the Kramers-Krönig analyzed optical conductivity of CrO_2 as a function of temperature, we have observed a narrowing of the cationic d-band gap from ~0.85 eV at 77 °K to ~0.5 eV at 450 °K. This has been interpreted as due to the disappearance of the long-range ferromagnetic order in this material as the temperature is raised through the Curie point. This suggests that correlation effects are not primarily responsible for the low-energy d-d transitions. Study of the optical reflectivity spectra of MoO_2 and WO_2 has revealed the similarities in the optical properties of these two materials despite the low dc conductivity of the latter. Comparison of the optical properties of all three oxides indicates a definite trend towards the broadening of the cationic d bands and increasing the band separation with increasing cationic radius. The observed trend is found to be generally consistent with that proposed by Wilson.[15] In all cases, no evidence is found for the existence of greatly differing bandwidths for the 3d bands in a given material.

ACKNOWLEDGMENTS

This work was supported in part by NSF Grant No. DMR 76-09091.

*Present address: Dept. of Physics, University of Sri Lanka, Peradeniya, Sri Lanka.

[1]D. S. Rodbell, J. M. Lommel, and R. C. Devries, J. Phys. Soc. Jpn. 21, 2430 (1966).
[2]D. B. Rogers, R. D. Shannon, A. W. Sleight, and J. L. Gillson, Inorg. Chem. 4, 841 (1969).
[3]L. Ben Dor and Y. Shimony, Mater. Res. Bull. 9, 837 (1974).
[4]L. L. Chase, Phys. Rev. B 10, 2226 (1974).
[5]I. Sadakata and E. Hanamura, J. Phys. Soc. Jpn. 34, 882 (1973).
[6]J. B. Goodenough, Prog. Solid State Chem. 5, 145 (1971).
[7]R. Srivastava and L. L. Chase, Solid State Commun. 11, 349 (1972).
[8]M. A. K. L. Dissanayake, Ph.D. thesis (Indiana University, 1977) (unpublished).
[9]A. S. Barker Jr. and J. P. Remeika, Solid State Com-

mun. 8, 1521 (1970).
[10]H. G. Reik, in *Polarons in Ionic Crystals and Polar Semiconductors*, edited by J. T. De Vreese (North-Holland, Amsterdam, 1972).
[11]V. N. Bogomolov, E. K. Kudinov, D. N. Mirlin, and Yu. A. Firsov, Sov. Phys. Solid State 9, 1630 (1968).
[12]K. Siratori and S. Iida, J. Phys. Soc. Jpn. 15, 210 (1960).
[13]L. A. Ladd and W. Paul, Solid State Commun. 7, 425 (1969).
[14]A. S. Barker Jr., H. W. Verleu, and H. J. Guggenheim, Phys. Rev. Lett. 17, 1286 (1966).
[15]J. A. Wilson, Adv. Phys. 21, 143 (1972).